Quaternary Geochronology 5 (2010) 644–656

Contents lists available at ScienceDirect

Quaternary Geochronology

journal homepage: www.elsevier.com/locate/quageo

Research Paper

The chronology of the late Lower Paleolithic in the Levant based on U–Th ages of speleothems from Qesem Cave, Israel

A. Gopher [a,*], A. Ayalon [b], M. Bar-Matthews [b], R. Barkai [a,1], A. Frumkin [c], P. Karkanas [d], R. Shahack-Gross [e,f]

[a] Institute of Archaeology, Tel Aviv University, 69978 Ramat Aviv, Israel
[b] Geological Survey of Israel, 30 Malchei Israel St., Jerusalem 95501, Israel
[c] Dept. of Physical Geography, The Hebrew University of Jerusalem, Jerusalem 91905, Israel
[d] Ephoreia of Palaeoanthropology–Speleology of Southern Greece, Ardittou 34b, 11636 Athens, Greece
[e] The Martin (Szusz) Dept. of Land of Israel Studies and Archaeology, Bar-Ilan University, Ramat-Gan 52900, Israel
[f] Kimmel Center for Archaeological Science, Weizmann Institute of Science, Rehovot 76100, Israel

ARTICLE INFO

Article history:
Received 11 December 2008
Received in revised form
26 February 2010
Accepted 22 March 2010
Available online 27 March 2010

Keywords:
Qesem Cave
Israel
Lower Paleolithic
Acheulo-Yabrudian complex
U-series dating

ABSTRACT

We present here the results of a U–Th dating project at Qesem Cave, a Middle Pleistocene, late Lower Paleolithic site in Israel. It provides 54 new MC-ICP-MS U–Th ages for speleothems from the cave. The results indicate that human occupation started sometime between ~420 and 320 ka and ended between 220 and 194 ka. A survey of dates from culturally similar sites in the Levant indicates that the general range of ca. 400–ca. 200 ka is an appropriate estimate for the life span of the Acheulo-Yabrudian Cultural Complex (AYCC).

1. Introduction

Qesem Cave was discovered on October 2000 following road construction, east of Tel-Aviv (Fig. 1) and assigned to the Acheulo-Yabrudian Cultural Complex (AYCC) of the late Lower Paleolithic. Stratigraphically, the Acheulo-Yabrudian complex of the Levant repeatedly appears above Lower Paleolithic Acheulian and below Middle Paleolithic Mousterian. Acheulo-Yabrudian sites are known from the central and southern Levant in caves and open air sites (Fig. 1). The AYCC was defined by Rust (1950) and is comprised of three major industries – Acheulo-Yabrudian, Yabrudian and Pre-Aurignacian/Amudian (Garrod, 1956, 1970; Jelinek, 1982, 1990; Bar-Yosef, 1994; Goren-Inbar, 1995; Copeland, 2000; Ronen and Weinstein-Evron, 2000). Two of its industries are noteworthy; the Yabrudian dominated by Quina scrapers; and the Amudian dominated by blades and shaped blades (tools).

The chronology of the AYCC was discussed by Bar-Yosef (1998), Copeland (2000) and Mercier and Valladas (1994, 2003). U-series, TL and ESR available ages indicate that the earliest dates for the Acheulo-Yabrudian are ca. 400 ka (Barkai et al., 2003; Rink et al., 2004; Le Tensorer et al., 2007a). The end of the AYCC is considered to be ca. 200 ka (Barkai et al., 2003; Le Tensorer et al., 2007a), although early work has indicated dates up to ~150 ka (e.g. Schwarcz, 1980; Grün et al., 1991; Farrand, 1994; Grün and Stringer, 2000; and see also Valladas et al., 1998).

The time span between 400 and 200 ka is an important chapter in the cultural and biological evolution of humans. This period includes early signs of, what is referred to in recent years as, modern human behavior. This pertains to behavioral patterns that are well established at Qesem Cave such as blade production – this is the dominant lithic technology throughout the Qesem Cave sequence (Gopher et al., 2005; Barkai et al., 2005); the habitual use of fire – exhibited at Qesem Cave (Karkanas et al., 2007); spatial activity patterning – apparently well established for Qesem Cave (Barkai et al., 2009); systematic hunting and butchering techniques and unique meat sharing habits (Stiner et al., 2009). Nothing is known of the hominids preceding the appearance of

* Corresponding author. Tel.: +972 3 6407607, +972 544 680192 (cell); fax: +972 3 6407237.
E-mail addresses: agopher@post.tau.ac.il (A. Gopher), ayalon@gsi.gov.il (A. Ayalon), matthews@gsi.gov.il (M. Bar-Matthews), barkaran@post.tau.ac.il (R. Barkai), msamos@mscc.huji.ac.il (A. Frumkin), pkark@eexi.gr (P. Karkanas), ruth.shahack@weizmann.ac.il (R. Shahack-Gross).
[1] Tel.: +972 3 6407607, +972 544 680192 (cell); fax: +972 3 6407237.

1871-1014/$ – see front matter © 2010 Elsevier B.V. All rights reserved.
doi:10.1016/j.quageo.2010.03.003

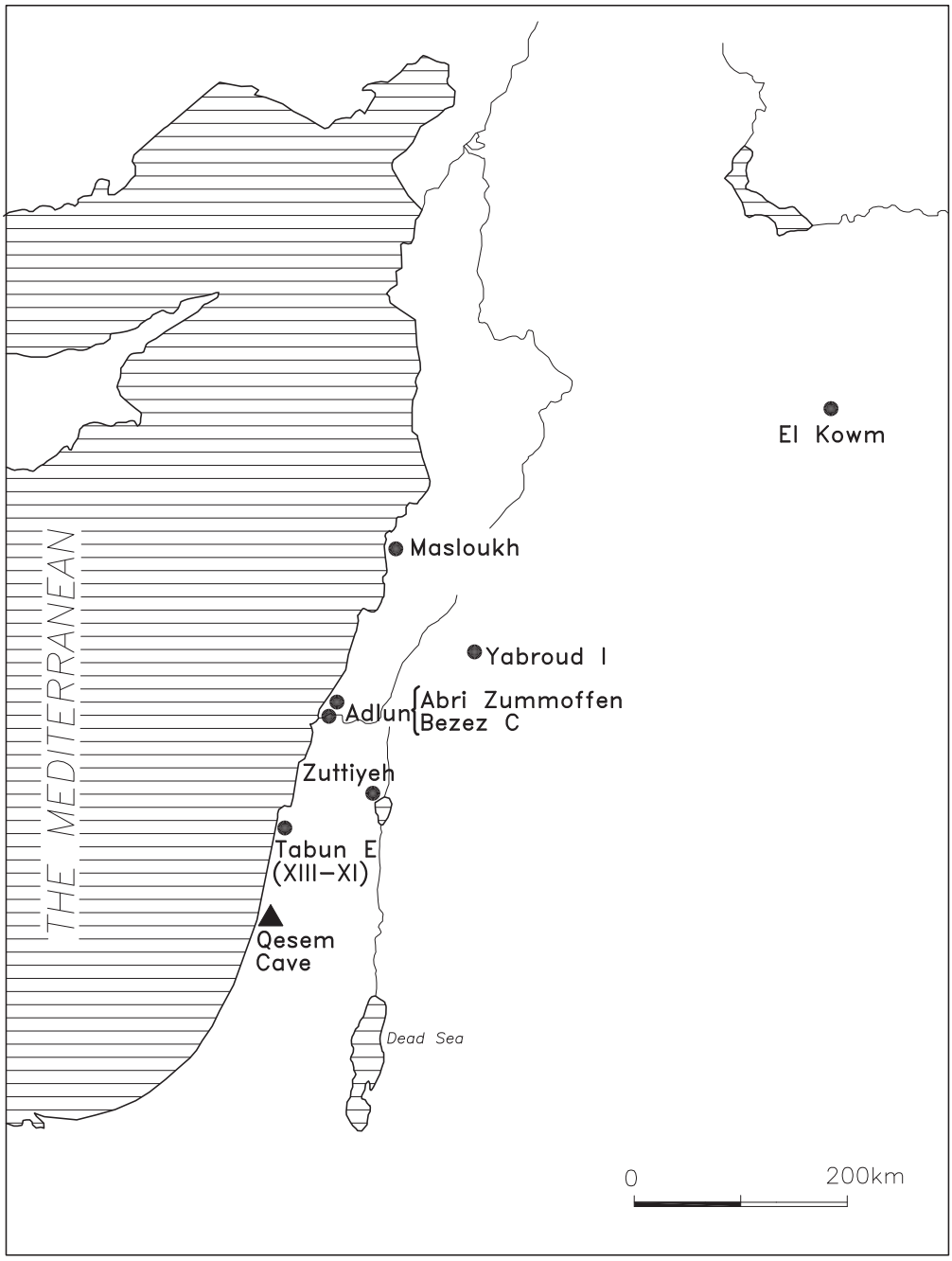

Fig. 1. Location map showing Qesem Cave and other AYCC sites mentioned in text.

Homo sapiens and the Neanderthals in the Near East, and a secure chronological framework for human remains at Qesem Cave (only teeth remains have been found so far) may be an important landmark en route to a better understanding of the evolution of modern humans. The dating of such an exceptionally well-preserved site of this age by U-series methods and additional methods (TL and ESR, currently underway) contributes significantly to better understanding of Middle Pleistocene human evolution.

A pilot U–Th speleothem dating project for Qesem Cave using thermal ionization mass spectrometry (TIMS) yielded 8 ages and indicated a general range between ca. 380 and 200 ka (Barkai et al., 2003). It was conducted during the preliminary stages of investigation at Qesem Cave and was limited in scope, focusing on only 8 samples extracted from one part of the cave. Despite these limitations, a comparison between archaeological finds and available absolute ages from Qesem Cave and from other AYCC sites supported this age range (Gopher et al., 2005).

To further constrain our understanding of the nature and timing of human adaptation and evolution during this important period, a series of field seasons were undertaken at Qesem Cave after 2004, in parallel with a continued program of U-series dating. Recent developments in our understanding of the site have emerged that require chronological constraint: (1) the recognition of two industries of the AYYC – the blade-dominated Amudian and the Quina scrapers dominated Yabrudian; (2) reassessment of the general stratigraphy and sedimentology (Karkanas et al., 2007) and the complex processes within the cave (Frumkin et al., 2009); (3) the discovery of human teeth in many different contexts throughout the caves sedimentological column.

To improve the Acheulo-Yabrudian chronology of Qesem Cave and add to the general framework of late Lower Paleolithic in the Levant, we sampled speleothem material for multi-collector inductively coupled plasma mass spectrometer (MC-ICP-MS) U–Th dating from a wider range of settings at Qesem Cave – some within archaeological sediments and some in clear stratigraphic correlation with archaeological horizons. These additional ages were necessary to investigate the representativeness of the previous age determinations and confirm the age range exhibited. The larger number of samples collected in the present study enabled us to examine whether occupation of the cave was continuous or was characterized by periods of desertion, etc. One drawback of the previous work (Barkai et al., 2003) was the indeterminate age of the end of human use (occupation) of the cave; this remained unsolved because the exact stratigraphic position of the youngest ages of the previous study (~152 ka) was not clear enough at the time. Subsequent excavation of the relevant areas in the cave enabled us to tackle this question by retrieving new stratigraphically well-constrained samples. A larger sample set also enabled more detailed investigation of U concentrations in the different samples to assess the possibility of open system behavior and the reliability of the ages obtained. The incorporation of micromorphological analyses of the analyzed speleothems and surrounding sediments also helped us address this issue.

2. Study site

2.1. The setting of Qesem Cave

Qesem Cave is located 12 km inland from the Mediterranean Sea, at an elevation of 90 m asl on the moderate western slopes of the Samaria hills above the channel of Wadi Rabah (Fig. 1). The area currently experiences a Mediterranean climate with annual average precipitation of 550–600 mm, however, the natural forest vegetation has long been destroyed by over-grazing and modern developmental projects.

The Samaria hills region is rich in karstic systems created by dissolution of the limestone, many of them still active. Qesem Cave is part of a larger karstic system within the limestone of the Bi'na Formation of the Cretaceous era. The system comprises of two adjacent (50 m apart) chamber caves with roughly similar dimensions – Qesem Cave and Kafr Qasem Cave (Frumkin et al., 2009). Both caves seem to have developed as isolated phreatic caves before the Samaria hills were uplifted to their present position (Frumkin and Fischhendler, 2005; Fischhendler and Frumkin, 2008), without a human-accessible entrance. Qesem Cave had been breached by natural erosion which allowed entry of hominins and associated deposition. Kafr Qasem Cave has been breached only by recent road-cutting. Since Kafr Qasem Cave still exists as an underground void with active natural cave processes, it was used as a model for reconstructing the history of Qesem Cave (Frumkin et al., 2009). Speleothem deposition in Kafr Qasem Cave (as well as in other nearby karstic caves) takes place in various settings and at various morphologies, such as cave pools, flowstone, stalactites and stalagmites. These are mainly composed of calcite, but aragonite also appears as a secondary speleothem mineral. In this study, all dated speleothems are composed of low magnesium calcite.

2.2. Lithic and faunal assemblages

After discovery of Qesem Cave, two short salvage seasons were conducted during 2001 and a new series of three field seasons followed in 2004–2006. The sedimentary column exposed was *ca.* 7.5 m thick, showing overlying anthropogenic horizons, each yielding rich lithic and faunal assemblages in fresh condition. The study of lithic technology and typology has shown that some of the assemblages are clearly dominated by blades, with many naturally-backed knives and shaped blades, including end-scrapers and burins, while, in other assemblages, blades were fewer (Barkai et al., 2009). A use-wear study of a blade-dominated assemblage has shown that blades were used mainly for cutting soft tissues – most probably for butchering animals (Lemorini et al., 2006). Sidescrapers appear throughout the stratigraphic sequence; single handaxes appear sporadically; and, several spheroids and chopping tools were found in Amudian assemblages of the lower sequence in the southern part of the cave. The blade assemblages seem to represent all stages of lithic manufacturing including raw material, cores, hammerstones, core trimming elements, blanks, waste material and shaped tools while in the case of scrapers and handaxes, only the end products are found in the cave. The emphasis on blade production in the assemblages led us to the conclusion that the site, as a whole, is to be assigned to the Amudian industry of the AYCC (Gopher et al., 2005; Barkai et al., 2005). However, we have recently modified this conclusion following the discovery of Yabrudian, scraper-dominated assemblages in specific parts of the cave (Barkai et al., 2009).

The faunal assemblages from all layers are dominated by fallow deer with some bovids, equids, pigs and turtles. Cut marks and burning signs were observed on a large portion of the bones (Stiner et al., 2009). Microfaunal elements recovered from some of the horizons show a rich variety of species and are under study now (Maul et al., in press).

3. Samples and methods

U-series ages of speleothems provide the most robust temporal constraints for archaeology in a karst setting. The dominant types of speleothem in Qesem Cave are calcite flowstone and pool deposits. Such deposits appear mainly in the eastern part of the cave. In the north-western part of the cave ("the shelf"), speleothem calcite appears as a matrix of cave breccia and on top of the shelf. While at Kafr Qasem Cave speleothem deposition continued throughout the entire last glacial cycle, most speleothem deposition within Qesem Cave apparently ceased in the last glacial period, possibly following the early opening of the cave, changes in cave roof, and associated changes in vadose flow routes (Ayalon et al., 1998; Frumkin et al., 1999, 2009). Some speleothem deposition did, however, continue as indicated by some of our U–Th ages (see Table 1).

Dating prehistoric cave sites using U–Th methods requires clear stratigraphic contexts to tie-in the dates obtained from the speleothems with the archaeological occupation layers. The strategy at Qesem Cave was to sample all parts of the sequence that provided speleothems. However, we had samples from the upper 4 m of the sequence, but no samples from the lower 3.5 m thick of the sedimentary sequence (for details on the sedimentary sequence at Qesem Cave, see Karkanas et al., 2007). We sampled speleothems from a variety of contexts – attached to the cave walls, on cave rocky shelves, or from within the occupational sediments. We focused on *in situ* samples and/or samples that can be related to the anthropogenic/archaeological sediments. We did not date speleothems in secondary deposition; however, fragments that dropped down, possibly off Q3, found within the archaeological layers below Q3, were dated in the first set (see Barkai et al., 2003, Fig. 2).

U–Th dating was undertaken by M. Bar-Matthews and A. Ayalon in the laboratories of the Geological Survey of Israel, Jerusalem and followed the method described in Vaks et al. (2006, 2007). Subsamples of 0.1–1.0 g of speleothem material were drilled using 0.5–4.0 mm diameter drill bits for U–Th analysis. All samples were

Table 1
U–Th results (concentration, activity ratios and age estimates) for calcite speleothems from Qesem Cave.

Sample no.	^{238}U conc. (ppm)	±2σ	$(^{234}U/^{238}U)_A$	±2σ	$(^{230}Th/^{232}Th)_A$	±2σ	$(^{230}Th/^{234}U)_A$	±2σ	Age		+2σ (ka)	−2σ (ka)
									Uncorrected (ka)	Corrected (ka)		
Q1a-bottom	0.2586	0.0003	1.0137	0.0042	341.6	4.0	0.9995	0.0125	556	550	320	150
Q1-middle	0.43	0.0004	1.0111	0.0020	997.6	6.0	0.9981	0.0064	550	550	160	100
Q1-top	0.2419	0.0002	1.0204	0.0037	147.9	2.0	0.9862	0.0082	420	420	60	50
Q2-top 1	0.2732	0.0004	1.0290	0.0041	14.8	0.2	0.9616	0.0070	332	320	30	30
Q2-middle	0.2301	0.0002	1.0317	0.0040	261.8	2.0	0.9449	0.0062	299	300	10	10
Q2-top 2	0.5936	0.0004	1.0610	0.0029	9.5	0.2	0.9273	0.0050	264	245	10	10
QA-06	0.41	0.0006	1.0271	0.0053	55.1	0.6	1.0373	0.0122	Indeterminate			
QE-06-1	0.2928	0.0011	1.0307	0.0040	42.4	0.74	0.9475	0.0164	304	300	30	30
Q3-1	0.1110	0.0002	1.0128	0.0044	14.6	0.2	0.9968	0.0132	521	510	240	140
Q3-2	0.2100	0.0004	1.0255	0.0073	33.9	0.4	0.9993	0.0145	496	490	240	130
Q3-3	0.1467	0.0003	1.0282	0.0051	40.1	0.6	0.9911	0.0166	430	425	110	80
Q3-4	0.1129	0.0002	1.0180	0.0034	21.7	0.4	0.9838	0.0141	412	405	85	65
Q3-5	0.0175	0.0002	1.0338	0.0070	58.2	3	0.9843	0.0213	392	390	105	80
Q3-6	0.1711	0.0002	1.0265	0.0060	35.0	0.6	0.9818	0.0176	392	385	80	70
Q3-7	0.1835	0.0011	1.0000	0.0141	26.6	0.8	0.9719	0.0144	388	380	120	85
Q3-8	0.2315	0.0002	1.0219	0.0036	38.7	0.4	0.9778	0.0088	383	380	45	40
Q3-9	0.1616	0.0002	1.0367	0.0086	46.2	0.6	0.9800	0.0133	374	370	65	55
Q3-10	0.2252	0.0002	1.0173	0.0060	20.2	0.2	0.9736	0.0096	374	365	55	45
Q3-11	0.0197	0.0002	1.0381	0.0053	6.5	0.2	0.9853	0.0166	390	360	85	70
Q3-12	0.2716	0.0013	0.9872	0.0144	22.1	0.6	0.9609	0.0151	356	355	105	75
Q3-13	0.1883	0.0002	1.0269	0.0063	96.3	1.2	0.9696	0.0124	353	350	45	40
Q3-14	0.1997	0.0002	1.0498	0.0061	34.3	0.6	0.9596	0.0175	316	310	40	35
Q3-15	0.2941	0.0002	1.0235	0.0020	7.2	0.2	0.9150	0.0149	261	235	30	25
Q3-16	0.2594	0.0006	1.0279	0.0042	8.5	0.2	0.9108	0.0199	255	235	30	30
Q3-17	0.2567	0.0004	1.0156	0.0024	5.4	0.2	0.9209	0.0175	270	230	40	35
Q3-18	0.4683	0.0004	1.0398	0.0014	25.1	0.4	0.8968	0.0113	238	230	10	10
Q3-19	0.3204	0.0004	1.0395	0.0028	120.3	3.8	0.8782	0.0259	222	220	25	20
Q3-20	1.28	0.0032	1.0312	0.0046	102.6	0.4	0.8251	0.0045	186	185	4	4
Q3-21	3.9	0.0274	1.0515	0.0070	46.8	0.6	0.7571	0.0097	151	148	6	5
Q3-22	3.9779	0.0053	0.9886	0.0015	265.8	1.6	0.7782	0.0035	165	164	2	2
Q3-23	6.5350	0.0060	1.0003	0.0016	299.2	1.6	0.7431	0.0033	148	147	2	2
Q3-24	7.9910	0.0240	1.0645	0.0035	41.0	0.34	0.8350	0.0061	189	185	6	6
Q3-25	1.1507	0.0013	1.0424	0.0022	36.4	0.2	0.9170	0.0053	258	255	10	10
Q3-26	1.1240	0.0008	1.0262	0.0019	26.3	0.2	0.8460	0.0042	200	195	5	5
Q3-27	9.1080	0.0160	1.0155	0.0024	11.8	0.2	0.8979	0.0040	244	230	10	10
Q3-28	5.4600	0.0400	1.0461	0.0062	69.1	0.4	0.8817	0.0066	223	220	7	7
Q3-29	0.4683	0.0004	1.0398	0.0014	25.1	0.4	0.8968	0.0113	238	230	13	12
Q3-06-Cover	0.4078	0.0002	1.0232	0.0026	56.0	0.6	0.8408	0.0089	197	194	7	7
Q3-06-Cover	0.4079	0.0002	1.0286	0.0026	66.8	0.6	0.8399	0.0091	197	194	7	7
Q4	0.3270	0.0002	0.9837	0.0019	11.0	0.2	0.2832	0.0050	36	31	2	2
Q5-bottom	0.4085	0.0004	1.0176	0.0020	2640	21	1.0025	0.0070	584	580	130	80
Q5-3	0.3153	0.0004	1.0130	0.0054	284.3	1.6	0.9928	0.0077	480	480	120	80
Q5-top	0.5431	0.0004	1.0255	0.0028	26.8	0.2	0.8812	0.0058	227	220	7	7
Q6-1	2.6827	0.0030	1.0178	0.0034	82.4	0.6	1.0023	0.0069	578	575	240	140
Q6-1b	0.3064	0.0002	1.0106	0.0033	11.5	0.2	1.0000	0.0070	591	575	240	140
Q6-2	0.2891	0.0004	1.0095	0.0027	215.9	1	0.9970	0.0045	543	540	140	90
Q6-2b	0.2038	0.0004	1.0215	0.0045	28.9	0.2	0.9995	0.0097	513	510	170	110
Q6-2c	0.2309	0.0004	1.0095	0.0045	23.5	0.2	0.9907	0.0114	473	465	130	90
Q6-2d	0.2238	0.0002	1.0144	0.0025	24.3	0.2	0.9895	0.0097	451	440	80	70
Q6-3	0.2477	0.0004	1.0127	0.0059	18.6	0.2	0.9825	0.0078	415	400	70	60
Q10	0.4114	0.0004	1.0095	0.0050	2.8	0.2	0.3190	0.0147	42	15	11	11
Q11	0.3525	0.0006	1.0374	0.0026	12.9	0.2	0.4966	0.0058	74	67	3	3
Q12	0.5045	0.0006	1.0500	0.0035	3.6	0.2	0.6840	0.0099	124	78	20	20
Q13	0.4462	0.0004	1.0357	0.0023	43.9	0.2	1.0253	0.0066	840	840	500	380

^{230}Th and ^{234}U half lives for age calculation are from Cheng et al. (2000).
Age corrected is based on $^{232}Th/^{238}U$ average atomic ratio of 1.8 ± 0.25 in the detrital components (Kaufman et al., 1998).
Uncertainty for ages >300 ka was calculated using Monte Carlo calculations (Ludwig, 2003) combined with the uncertainty in $^{232}Th/^{238}U$ value of ±0.25.

totally dissolved, with a combination of 7 M HNO_3 and HF, and spiked with a mixed $^{229}Th/^{236}U$ spike. The reproducibility of $^{234}U/^{238}U$ ratio was 0.11% (2σ). The sample was loaded onto mini-columns that contained 2 ml Bio-Rad AG 1X8 200–400 mesh resin. U was eluted by 1 M HBr and Th with 6 M HCl. U and Th solutions were evaporated to dryness and the residue dissolved in 2 ml and 5 ml of 0.1 M HNO_3 respectively. U–Th dating was performed using a Nu Instruments Ltd (UK) MC-ICP-MS equipped with 12 Faraday cups and 3 ion counters. Each sample was introduced to the MC-ICP-MS through an Aridus® micro-concentric desolvating nebuliser sample introducing system. The instrumental mass bias was corrected (using exponential equation) by measuring the $^{235}U/^{238}U$ ratio and correcting with the natural $^{235}U/^{238}U$ ratio. Calibration of ion counters relative to Faraday cups was performed using several cycles of measurement with different collector configurations in each particular analysis (Vaks et al., 2006).

Isotope ratios are given in Table 1 as activity ratios with 2σ uncertainties. The errors are propagated from the in-run precision errors, weighing errors and uncertainties in spike concentrations and isotopic compositions. The ^{230}Th and ^{234}U half lives are taken from Cheng et al. (2000). Uncertainties in the half lives of the U-series isotopes are not included in the error propagation.

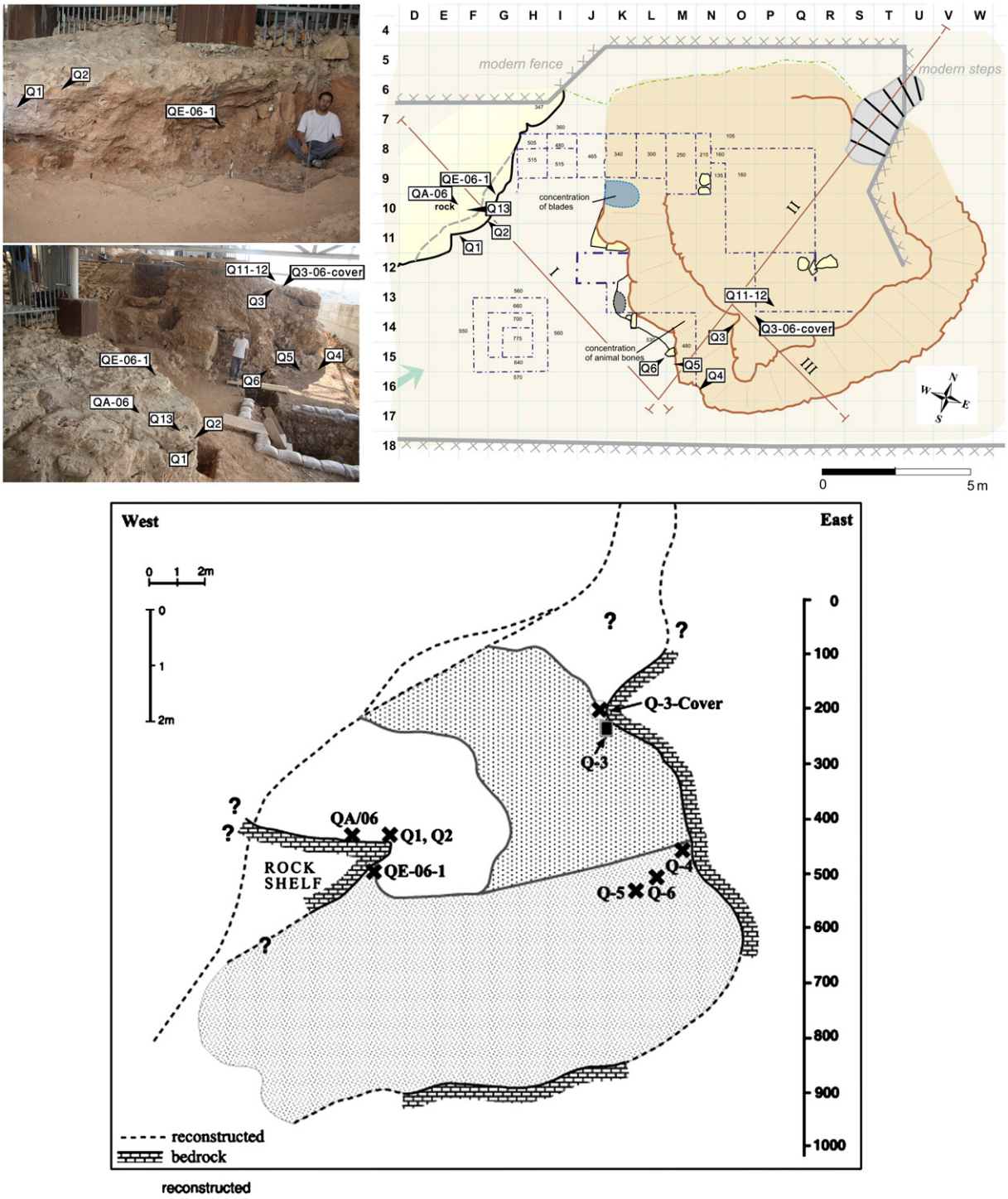

Fig. 2. Bottom left: a general view of the cave looking east–north–east indicating the location of samples; top left: a closer look at the location of the shelf samples; top right: a plan of the cave showing horizontal location of the dated samples and the lines along which the section in lower right was made; bottom right: a schematic section showing vertical position of samples. It is presented as a west–east section looking north and compiles (to scale) the west–east line I, the east–north–east line II, and an extension towards the eastern cave wall, line III shown in the plan. Note, for example, that the void below sample Q3 mentioned in text does not show in the section since there are sediments in similar elevations to the north of it. Note difference between the vertical and horizontal scales in the section.

The U–Th method assumes that all ^{230}Th present in the calcite speleothem is formed *in situ* by radioactive decay of uranium that co-precipitated with the calcite. However, this component is often accompanied by detrital material such as clays, oxides and hydroxides (e.g. Richards and Dorale, 2003; Kaufman et al., 1998). For correction, a ^{232}Th/^{238}U atomic ratio of 1.8 ± 0.25 in the detrital components was used (this value was measured using an isochron method for speleothems located in Upper Cretaceous carbonate host rocks from central Israel, Kaufman et al., 1998). The error on the corrected ages combines the error on the uncorrected ages together with the uncertainty of ±0.25 on the ^{232}Th/^{238}U ratio of 1.8 in the detrital component.

An additional possible source of contamination considered in dating the Qesem Cave speleothem samples is U transfer from dissolution of bone and teeth with very high U content (up to 100 ppm, Pike and Pettitt, 2003) in direct contact, or close to the dated samples. If this was the case, addition of U would give rise to open system behavior and ages would not represent the 'real' age of speleothem formation. Such contamination may be relevant to a series of 10 samples, all composed of low magnesium calcite, Q3-20/29 (see Table 1), that have exceptionally high U concentration (see below). Similar processes of contamination may also occur as a result of the presence of bat guano (Shahack-Gross et al., 2004). One way to assess the influence of an open system on the reliability of the ages is to examine if the ages are in correct stratigraphic order. In this study, it is shown that the ages of speleothems with high U concentrations are not in stratigraphic order (Table 1, sample Q2).

4. Results

Ages for Qesem Cave, uncorrected and corrected for initial Th, are presented in Table 1. Ages referred to in text below are corrected ages. The 54 ages presented here include the 10 samples (Q3-20/29) that have anomalously high U concentrations. We accompany the presentation of the ages with descriptions of sample location and context within the cave.

4.1. The shelf

Samples Q1, Q2, QA-06, QE-06-1 and Q13 are from a rock shelf situated about 4 m above the base of the cave and over 3 m below the top of the occupational sediments. We note that it is possible that sediments lower than the shelf were older, coeval or later than the deposits on the shelf itself (and see Q3 below). The shelf consists of a geological breccia that accumulated as breakdown debris of bedrock cemented by speleothem deposits (Fig. 2). Speleothems continued to be formed *in situ*, probably in small pools of saturated water, indicated by flat horizontal bedding of the speleothem calcite. The shelf includes some evidence of human presence in the form of cemented sediments that include animal bones and stone artifacts attached to the shelf's surface.

Sample Q1 is a horizontally-bedded pool-calcite deposit at the eastern part of shelf at elevation 423–427 cm below datum, facing the main chamber of the cave. It is located below the archaeological sediments that are cemented to the shelf and has no physical contact with them (Fig. 2).

The ages of this sample are close to the limit of the U–Th method and age uncertainties are therefore large, but the ages are in stratigraphic order (see Table 1). The dates range between ages older than 550 + 320/−150 ka (Q1a-bottom) at the bottom, 550 + 160/−100 ka (Q1-middle) in the middle part and 420 + 60/−50 ka (Q1-top) at the top of the speleothem. Several other samples from the bottom part of this speleothem yielded ages older than the U–Th dating method range; i.e. older than ~550 ka. Uranium concentrations in these samples range between 0.24 and 0.43 ppm (Table 1), typical for speleothems, thus we consider these ages to be reliable.

Sample Q2 (Fig. 2) is located 40 cm to the north of sample Q1 within the same general setting at elevation 414–421 cm below datum. The Q2 speleothem calcite is interbedded with cemented archaeological sediments, animal bones and flint artifacts (Fig. 3).

The 3 ages obtained for Q2 (Table 1) are 320 ± 30 ka (top 1), 300 ± 10 ka (middle) 245 ± 10 ka (top 2) – much younger than Q1. Because Q2 is actually an interbedding of speleothem material with archaeological finds, the ages may be seen as direct indicators for archaeological occupation between ca. 319 and 245 ka. Within error, samples Q2-top 1 and Q2-middle show similar ages. The age of sample Q2-top 2 is younger and it shows a higher U concentration of ca. 0.6 ppm compared with the 0.2–0.4 typical of the other two samples, and to other speleothems from Qesem Cave. It is possible that this younger age is a result of an "open system" due to U addition after leaching from the bones.

Fig. 3. Sample Q2 (width of saw cut ca. 10 cm).

Sample QA-06 is a speleothem located slightly to the north of sample Q2 in contact with a patch of cemented sediments including archaeological finds. This sample produced an indeterminate age, beyond the limit of the U–Th dating method.

Sample QE-06-1 is a speleothem crust (2–3 cm thickness) found in Square G/9c at elevation 470–480 cm below datum within orange-colored archaeological sediment (Fig. 4) under the eastern part of the shelf, facing east. Micromorphological analysis was carried out on a sample that includes the speleothem and 3 cm of sediment accumulation just below it. The results show that the sediments immediately below the speleothem crust include wood ash, bones and flint chips (Fig. 5c). The amount of sparitic calcite increased from bottom to top (Fig. 5b), forming massive, pure speleothems at the uppermost part of the sample (Fig. 5a). These observations indicate that the speleothem formed at the time the archaeological sediment was deposited or shortly after, thus implying that the archaeological sediment below the speleothem is not reworked but preserved *in situ*. A few other micromorphological samples from various locations in the cave do include reworked sediments whose microscopic appearance is quite different from the material of the sample discussed here. The speleothem itself does not show signs of dissolution or re-precipitation. The date obtained from this speleothem is 300 ka + 30/−30 ka (Table 1) and it provides a minimum age for the 3.5 m of the sediment sequence

Fig. 4. QE-06-1 below the shelf.

below it. This sample unequivocally shows that anthropogenic sediments and thus human activities in the cave occurred below the shelf prior to, and after ca. 300 ka.

Sample Q13 is on the shelf in contact with archaeological hardened sediments, near Q2. The age, as in the case of QA-06, is beyond the limit of the dating method.

We summarize the shelf evidence as follows:

- Despite the large uncertainties on the older ages, the difference between samples is significant and they are in correct stratigraphic order.
- The build up of the shelf itself started early, at ages beyond the range of the dating method as indicated by the dates of lower Q1 (older than 550 ka). This phase occurred most likely before the cave had an opening to the surface. The upper part of sample Q1, close to the shelf surface is dated to ~550–420 ka.
- When human occupation at the cave had started, animal bones and stone artifacts were incorporated into the cave's deposits in the lower depositional sequence (Karkanas et al., 2007) and on the shelf. The dates obtained from speleothem Q2 interbedded with archaeological material, range between 320 and 245 ka.
- Sample QE-06-1 taken from within the anthropogenic sediments just below the shelf was dated to ~300 ka thus indicates human occupation in this part of the cave before and after ~300 ka.

Based on the ages of Q1 and Q2 together, the occupation of the cave, on the shelf, started after 418 and not later than 319 ka and continued up to 245. Based on the age of sample QE-06-1, occupation below the shelf indicates human activity around 300 ka. The 3.5 m of occupational sediments below QE-06-1 must be older.

4.2. Q3 flowstone and speleothem crusts above it

Sample Q3 is a massive flowstone located on the eastern wall of the cave in square Q/14c (Fig. 2) at elevation 225–245 cm below datum. This is a large calcitic flowstone that was deposited by a thin film of water flowing over an inclined cave surface of a positive gradient (i.e. not under the negative slope just below the ceiling; Frumkin et al., 2009). CO_2 degassing along such a surface is efficient due to the high surface area:volume ratio of the water, allowing deposition of thick flowstone layers, which normally comprise most of the speleothem volume in caves.

The unconsolidated cave deposits underlying Q3 and sample Q5-top (located some 3 m below Q3 showing a date of ca. 220 ka,

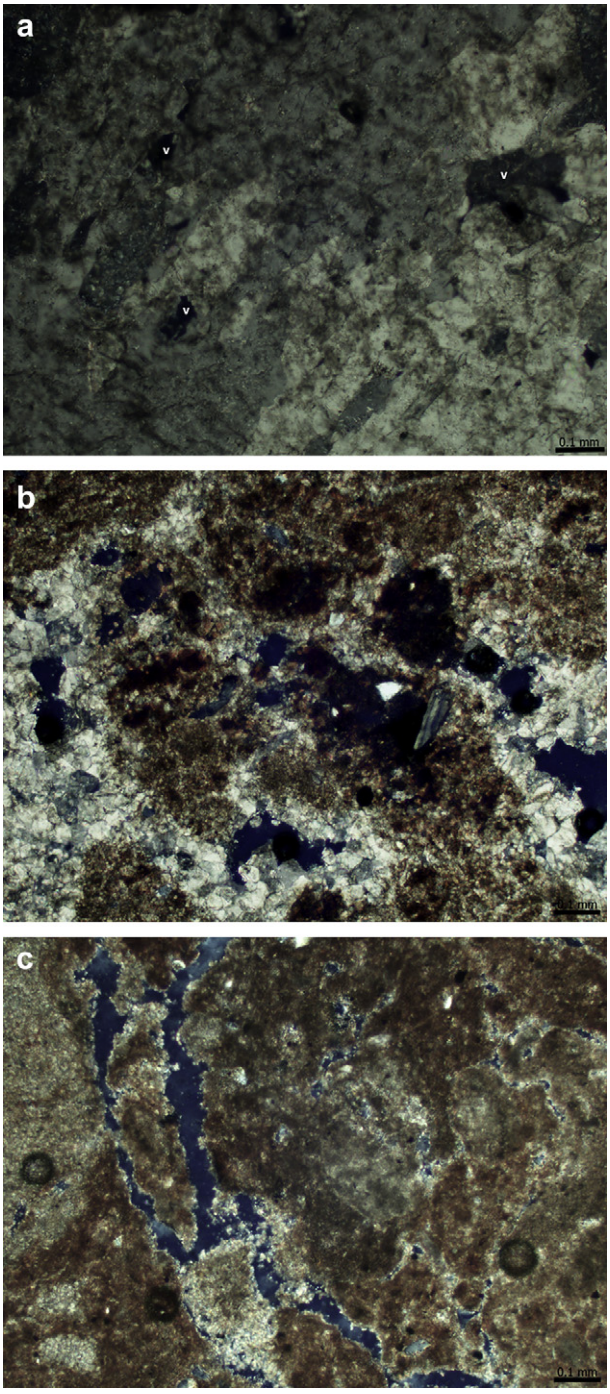

Fig. 5. Thin section of sample QE-06-1. Photomicrographs show the micromorphology related to speleothem QE-06-1. All microphotographs are in crossed polarized light. (a) The pure speleothem composed of large sparitic calcite crystals. (b) The sediment immediately below the speleothem showing impregnation by sparitic calcite as carbonate-rich solution moved downwards from the speleothem to the sediment below it. (c) ca. 5 cm below the bottom of the speleothem, showing reworked ash-containing sediment.

see below and Table 1) indicate that Q3 formed a hanging ledge on the cave's wall, while the main void of the cave extended west and below it. That is to say that it is possible that deposition of speleothem Q3 and anthropogenic sediments in the void below Q3 was coeval. Furthermore, flowstone Q3 started forming as early as 508 ka + 244/−136 ka, an age with a large error and may suggest that it was deposited earlier, and the latest reliable date obtained

from this flowstone is 220 ka + 23/−21 ka (see below). Because this age is younger than those obtained from the shelf speleothems that were associated with archaeological finds, it is clear that the formation of Q3 overlapped with human occupation, although not throughout the ca. 250 ka represented by this flowstone. Anthropogenic sediments thus accumulated below Q3 until they reached its base and later covered it. The archaeological deposit that accumulated conformably above the Q3 flowstone clearly postdates it.

The major component of the age data set for Q3 was derived from a saw-cut section of the thick intact flowstone (Fig. 6). The flowstone includes three major visible parts – lower, middle and upper. The middle part is the thickest. The upper part of Q3 is composed of a mixture of the speleothem and archaeological finds including flint and bone [i.e. the speleothem material cemented the archaeological deposit] (Fig. 6)]. In addition, a thin flowstone crust has been identified (east and north of top Q3) above Q3 (termed Q3-06-COVER), separated from top Q3 by 20 cm of archaeological sediment (i.e. at elevation ~205 cm below datum). This crust is the uppermost deposit exposed in the cave's stratigraphic section, setting a terminus for the latest human use of the cave (Fig. 7).

The total number of analyses on Q3 presented here is 29; 19 speleothem sub-samples were from the lower and middle parts of Q3 (Fig. 7) and 10 sub-samples were from the upper part of Q3, in close proximity, direct contact, or within the archaeological layer. Two additional samples were from Q3-06-COVER.

The ages obtained for the lower part of Q3 range between 510 ka + 240/−140 ka and 350 ka + 45/−40 ka over a thickness of 100 mm (see Table 1, Q3-1/13). A break in deposition separates the lower from the middle part of Q3. This break may indicate a hiatus (either lack of deposition or erosion). The calcite underlying this break dates to 310 ka + 40/−35 ka (Table 1, Q3-14) while the available ages above the break (middle part of Q3), range from 235 ka + 30/−25 ka to 220 ka + 25/−20 ka, over a thickness of ~50 mm (see Table 1, Q3-15/19). It is important to emphasize that

Fig. 6. Q3 – a saw-cut sample showing sample QCB-20.

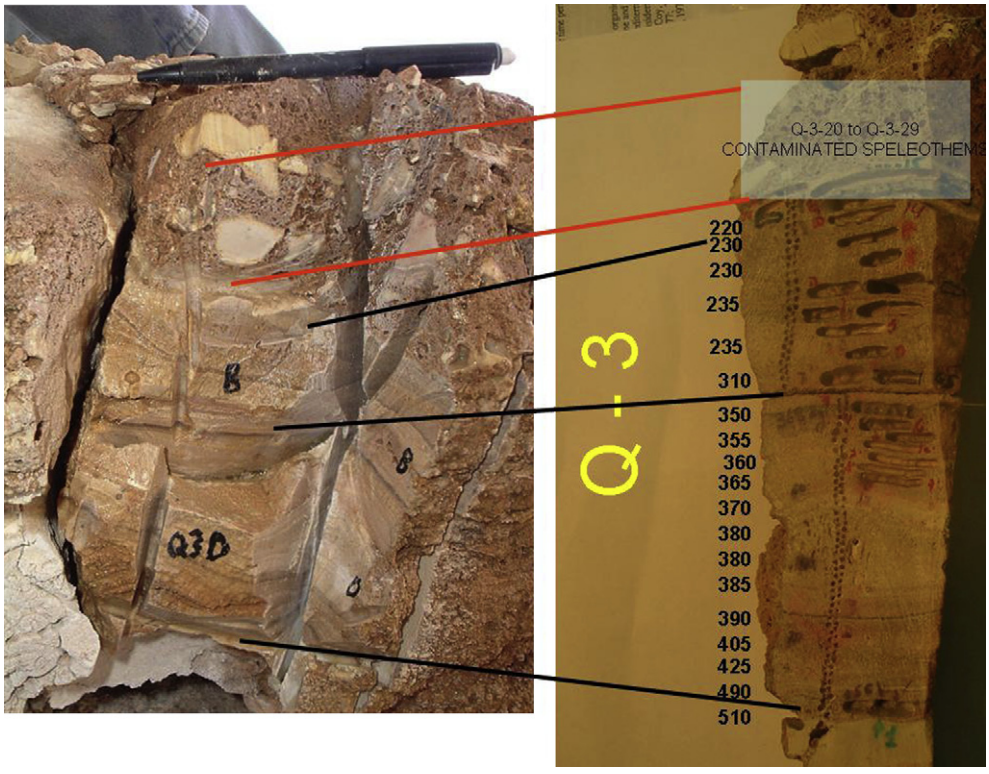

Fig. 7. Q3 – showing the mean ages and the sub-sample locations. White box shows the area suspected of contamination. Black lines indicate obvious breaks in deposition.

uranium concentrations in the lower and middle parts, above and below the break vary between 0.1 and 0.5 ppm (see Table 1). The ages accord with the stratigraphic order indicating a normal setting with no disturbance.

Ages obtained from the upper part of Q3 (Table 1, Q3-20/29) range between 255 ± 10 ka and 147 ± 2 ka. These 10 dates do not accord with the stratigraphy of the speleothem's laminae and their U concentrations range from 1 to 9 ppm, which is much higher than the normal range of Qesem Cave speleothems. The proximity and/or contact of these samples with U rich bones and teeth, and a possible chemical reaction between bone, teeth and the carbonate (leaching or adding of elements into the carbonate) may have lead to an enriched U concentration in the speleothem. The ages of the uppermost part of Q3 may thus reflect secondary processes – i.e. an open system.

In order to ascertain whether the high U concentrations in this part of the speleothem are from weathering bones or other processes, we sampled the upper part of Q3 with the sediment above it for a micromorphological examination (sample QCB-20) (Fig. 6). The speleothem part of sample QCB-20 shows clear signs of dissolution and re-precipitation of calcite indicating that the system was indeed open. The uppermost 0.5–1.0 mm of the speleothem is a thin "dirty" film composed of clay and phosphates (Fig. 8, arrows). The archaeological sediment above this film is composed of clay, calcite, bone fragments and patches of micritic calcite, phosphate nodules, and manganese-oxide "flowers". No signs of bone dissolution were observed. Using fluorescence microscopy in which phosphate was excited showed penetration of phosphate-rich solutions from the top of the speleothem downwards, mostly following vertical dissolution voids (Fig. 8) – i.e. the solutions were acidic. The source of phosphate-containing acids in caves is usually from degrading bat guano (Shahack-Gross et al., 2004). We therefore suggest that the top part of Q3 was dissolved due to roosting activities of bats above it. We should note that the area below the Q3 flowstone yielded rich assemblages of microvertebrate bones most probably deposited by birds of prey (Maul et al., in press). The micromorphological data together with the high U concentrations and the lack of stratigraphic order in the dates thus indicate that the upper part of Q3 was contaminated by uranium due to dissolution and re-precipitation processes.

Note that in the early set of dates on Q3 (Barkai et al., 2003), the youngest speleothem laminae below the uppermost archaeological layer had a U concentration of 1.7 ppm, which is significantly above the normal range, and consequently gave a young age of 207 ka. Following our intensive re-dating of Q3 we may conclude that this age too (like the new dates Q3-20/29) does not represent primary deposition processes.

Two additional age determinations are related to Q3 by name although they are not part of the Q3 flowstone. These are made on a speleothem crust covering the top of the archaeological sediments ca. 1.5 m east and north of Q3 in squares O/14b,d at elevation 205 cm below datum (Figs. 2 and 9) and were named Q3-COVER (Table 1). Both ages are ~194 ± 7 ka. The U concentration of these samples was within the normal range for carbonate speleothems and therefore considered reliable.

Summarizing the dates of Q3 and related samples:

- Dates # Q3-1/19 are in correct stratigraphic order and their U concentrations are low representing a reliable long depositional period of 290 ka of flowstone Q3. On the other hand, the ages of samples Q3-20/29 are not reliable because (1) their U content is higher by an order of magnitude compared to other Q3 laminae in particular, and compared with other speleothems from Qesem Cave in general, and (2) lack of stratigraphic order. This was caused by an open system, associated with dissolution and re-precipitation, of phosphate-rich solutions that also included U. The youngest reliable date of Q3 flowstone is thus ~220 ka.
- The deposition of Q3 occurred between ~510 and 220 ka, with an apparent hiatus between ~310 and 235 ka. This hiatus in speleothem deposition can be attributed to local change of conditions, such as temporary clogging of the fissure supplying water (i.e. lack of deposition) or increased aggressivity of the water (i.e. erosion/dissolution). A more general or regional explanation for this hiatus, such as a long dry period is unlikely. First, because other Qesem Cave ages fall between 310 and 235 ka: Q2 (300 and 245 ka) and QE-06-1 (300 ka). And, secondly, speleothems dated to ~300–275 ka at the Ma'ale Efrayim Cave east of Qesem Cave (Vaks, 2008) were probably deposited by rainfall systems coming from the eastern

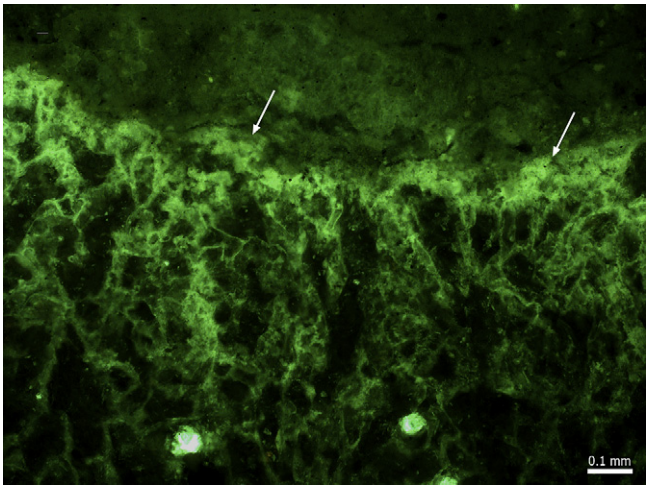

Fig. 8. An autofluorescence image of sample QCB-20 showing phosphatized calcite at the top part of speleothem Q3. The arrows indicate the junction between the speleothem and the sediment above it. Note that the junction surface is highly phosphatized relative to the sediment above the speleothem. Also note the semi-vertical penetration of phosphate downwards into the speleothem along voids/cracks. Microphotograph taken using blue light (using filters for excitation at 420–450 nm and suppression at 520 nm). Arrows show the uppermost 0.5–1.0 mm of the speleothem – a thin "dirty" film composed of clay and phosphates.

Fig. 9. Q3-06-COVER: A speleothem crust covering the top of the archaeological sediments ca. 1.5 m east and north of Q3 in squares O/14b,d at elevation 205 cm below datum.

Mediterranean passing through the Qesem Cave area (Vaks et al., 2003).

- The archaeological deposit overlying Q3 is constrained by the underlying youngest reliable age (220 ka) and the Q3-06-COVER (194 ka) covering this latest archaeological deposit on-site. The cave was thus eventually deserted during this time interval.

4.3. Other samples

Sample Q4, below Q3 attached to the eastern cave wall at elevation 470 cm below datum consists of white cave deposit common to cave walls, often referred to as "popcorn" (Fig. 2). This sample is young, ~31.0 ka (Table 1) and is not relevant to the time period discussed here.

Sample Q5 is a stalagmite near the eastern wall of the cave below Q3, at elevation 532 cm below datum (Fig. 2). It was sampled in order to try to estimate the date of the change in sedimentation between the lower and upper sedimentary sequences (Karkanas et al., 2007). Three ages were determined and they range from older than ~580 ka + 130 and −80 ka (Q5-bottom) to 480 + 120/−80 ka (Q5-3) and ~220 ± 7 ka (Q5-top) (Table 1).

Sample Q6 is a flowstone deposit on a stone block, 0.5 m north of Q5, below Q3 at elevation 505–510 cm below datum, underlying archaeological sediments near the eastern wall of the cave (Fig. 2). Seven laminae have been dated, ranging between 576 ka (unreliable date with high U concentration) and 400 + 70/−60 ka (Table 1). It is not clear whether it was *in situ*.

Sample Q5 and to a degree Q6 also are located at elevations close to the border between the lower and upper sedimentation sequences of Qesem Cave (Karkanas et al., 2007). The large range of dates from these samples does not enable the estimation of an age for the change in sedimentation between the two sequences. However, the fact that such old stalagmites formed close to the contact of the two sequences indicates that the cave's surface was irregular, probably forming a topography similar to that observed today, i.e. the eastern part of the cave and the shelf on the west were elevated surfaces at the same time that the middle part of the cave was a low. Even if Q5 and Q6 fell from above and are not *in situ*, they must have needed a space to fall into – i.e. there was open space below Q3.

Sample Q10, outside the cave, contains a high concentration of detrital material and yielded an age of 15 ± 11 ka (Table 1). Samples Q11 and Q12 are both above the latest archaeological sediments, they provide late dates not relevant to our discussion. Q11 is a speleothem crust covering the uppermost archaeological layer, just above burnt flint and bones. The sample is in contact with the archaeological material but the young age (67 ± 3 ka, Table 1) indicates that it formed after human occupation in the cave ceased. Q12 is a speleothem crust above the archaeological layer near Q11 but with no archaeological remains. The speleothem contains a high concentration of detrital material and the age (78 ka ± 20 ka, Table 1).

4.4. Summarizing the Qesem results

Although our U-series dating program is comprehensive, there are gaps in the chronological sequence. Unambiguous dates for human occupation range from 320 to 245 ka based on samples Q2 and QE-06-1. Human occupation could, however, have started at any time between 420 and 320 ka. Occupation continued until between 220 and 194 ka, when the cave was altered to a degree that did not favour human occupation.

A U–Th age of 218 ka for a speleothem fragment within the sediments below Q3 (see Barkai et al., 2003) may indicate occupation at this time also, or end of occupation and collapse causing this speleothem to become broken.

5. Discussion

5.1. Stratigraphy of the Acheulo-Yabrudian Cultural Complex

The stratigraphic position of the AYCC in the Levant (Israel, Lebanon, and Syria) is quite clear – between the Lower Paleolithic Acheulian and the Middle Paleolithic Mousterian. At key sites such as Tabun Cave, Umm el Tlel and possibly Bezez Cave, the Acheulo-Yabrudian layers are sandwiched between Acheulian and Mousterian layers. This may also be the case of Jamal Cave. At Nadaouiyeh Ain Askar the Acheulo-Yabrudian appears on top of the Acheulian and a possible similar case, although not fully clear is the cave of Masloukh. At Yabrud I and other sites, such as Hayonim Cave, Misliya, Dederiyeh, Hummal and most probably in the cave of Zuttiyeh too, Acheulo-Yabrudian layers are positioned below Mousterian occupation layers. Sites with Acheulo-Yabrudian only and no earlier or later occupations include Qesem Cave and Abri Zoumoffen. This extensive data set, accumulated during the past 80 years of Paleolithic research in the Levant, clearly bears out the post-Acheulian/pre-Mousterian stratigraphic position of the Acheulo-Yabrudian Cultural Complex.

5.2. Geochronology of the Acheulo-Yabrudian Cultural Complex

The scarcity of absolute dates for the Lower and Middle Paleolithic in the Levant including the AYCC seems to be partly amended in recent years with new dates presented. There are, however, other problems, especially with dates published in the early stages of TL, ESR and U-series dating. One problem is that dating intensity in the different Lower and Middle Paleolithic sites is highly variable (e.g. rich in Tabun and Hayonim caves, poor in Yabrud I, Zuttiyeh, Revadim or Holon). Another problem is that some of the sites mentioned were TL and ESR dated without on-site dosimetry. An additional issue is that some of the samples of burnt flint or animal teeth originated in stored collections of finds from old excavations (e.g. Yabrud I, some of the Tabun dates, Zuttiyeh, Umm Qatafa, Holon). And lastly, there is a problem of context reliability – some TL and ESR sample locations within site stratigraphies are unclear (Zuttiyeh, some of the Tabun samples and possibly Umm Qatafa too). In the Acheulian case of Holon, some of the dates were made on samples from a newly excavated trench off the originally excavated layers, and in the case of Revadim, a calcitic encrustation attached to flint tools was dated rather than speleothem calcite. We present below a critical view of the available dates.

5.2.1. AYCC dates

The AYCC can be generally dated to a range from ca. 400 to ca. 200 ka by a small number of reliable ages currently available.

Tabun Cave provides a few sets of dates. A combined ESR/U-series age for layer Ed, the base of the AYCC layer, is close to 400 ka (Rink et al., 2004). TL dates of Tabun showed a range from 330 to 270–260 ka for layer E (Mercier et al., 1995). However, Schwarcz and Rink (1998) claim that Mercier et al. (1995) dated Tabun E between 386 ± 33 ka and 278 ± 34 ka. Additional ESR and U-series dates for Tabun E were discussed by Grün et al. (1991) and McDermott et al. (1993) showing a range between 205 and 160 ka for this layer. Later, Grün and Stringer (2000) re-evaluated these results and dated Tabun E from 208 ± 102 ka to 44 ka – obviously a wide range that is difficult to interpret. A later reassessment of Tabun TL chronology by Mercier and Valladas (2003) has set the boundary between Tabun E and D somewhat earlier than 250 ka.

Jamal Cave, adjacent to Tabun Cave yielded U–Th dates around 225 ka on a flowstone above the Acheulo-Yabrudian layer (Weinstein-Evron et al., 1999). It is thus clear that the AYCC of Jamal Cave predates 225 ka.

Syrian sites of the Acheulo-Yabrudian Cultural Complex first provided U-series dates younger than 200 ka for Hummal and Umm el Tlel (Hennig and Hours, 1982). TL dates for Hummal by the Oxford Research Laboratory (1990) in the order of ca. 160 ka were criticized by Mercier and Valladas (1994). The most recent summaries on Hummal based on the available TL dates suggest a range in the order of 422 ± 55–243 ± 40 ka for the AYCC and 220–150 ka for the Tabun D-like Hummalian (Le Tensorer et al., 2007a,b).

Two sites of importance to the history of Acheulo-Yabrudian research, Zuttiyeh and Yabrud I, were not intensively dated. The Th/U dates from Zuttiyeh (see Bar-Yosef, 1998: 46; Table 1 quoting Schwarcz, 1980) are all younger than 200 ka. TL dates from Zuttiyeh are all from the Mousterian layers, the oldest being 157 ka (Valladas et al., 1998). The Yabrud I TL dates (Mercier and Valladas, 1994) cluster around 200 ka. Other Yabrud I dates include ESR from Solecky's layers 18/19 with average dates of 222 ka (using the early uptake); 226 ka (by the combination uptake) and 256 ka (by the linear uptake) (Porat et al., 2002).

In summary, the dates from Tabun and Jamal Caves and those of Hummal seem to clearly show a range that can be generally summarized as 420–225 ka. The other dates from Tabun, Hummal, Yabrud I and Zuttiyeh, mostly from the early stages of absolute dating, or suffering from the problems mentioned above, suggest a younger chronology for the Acheulo-Yabrudian Cultural Complex.

The Qesem Cave ages are a significant contribution to the ever-growing database of radiometric ages of the AYCC in the Near East. Although it is not fully clear when the AYCC occupation at the cave started, our data suggest it occurred before 320 ka, and probably quite earlier if we consider preliminary, yet unpublished TL dates. The end of the AYCC occupation at Qesem Cave was between 220 and 194 ka, may be closer to 220 ka as indicated by the 218 ka date on a broken speleothem within the sediments below Q3 (see above and Barkai et al., 2003).

5.2.2. Acheulian dates

The absolute chronology of Acheulian sites in the region is sparse and not always directly related to the Acheulo-Yabrudian but it may still provide a post quem date for the Acheulo-Yabrudian. Gesher Benot Ya'aqov known to have been occupied between 800 and 700 ka (including the Bruns/Matuyama paleomagnetic boundary) was recently ESR dated to ca. 650 ka (corrected by rate of sedimentation to ca. 750 ka) by Rink and Schawrcz (2005). The Acheulian Evron Quarry yielded luminescence and ESR dates in the order of 630–330 ka (Porat and Ronen, 2002). The Acheulian layer of Umm Qatafa first yielded young U-series dates (Schwarcz, 1980). Later, layer D2 was ESR dated showing averages of 262 (by the early uptake), 313 (by the combination uptake) and 409 (for the linear uptake) (Porat et al., 2002). They argue that the combination uptake dates for one of the teeth is the most reliable and concluded that the Acheulian layer D2 ended at around 213 ± 26 ka. The Acheulian site of Revadim (Marder et al., 1999) shows luminescence dates between 403 and 194 ka, but it is not clear how the dates relate to the human occupation. U–Th dates on calcitic crusts attached to flint artifacts resulted in dates exceeding 400 ka (Marder et al., 2007) that might be later than the artifacts themselves. The Acheulian site of Birket Ram (Feraud et al., 1983) clearly predates 233 ka and postdates 800 ka but the date of the occupation is not clear.

Porat et al. (1999, 2002) and Porat (2007) suggest on the basis of ESR and luminescence ages, a date for Acheulian Holon around 200 ka (215 ± 30) and a rapid Lower–Middle Paleolithic (Acheulian–Mousterian) transition at around that date. The ESR dates were made on teeth collected in the Noy excavation of the 1960s and the luminescence dates on samples extracted from one of two newly excavated trenches, some 8–10 m away from the original Noy excavation area (Porat, 2007: 27 and Fig. 3.2). We support the reservations made by Rink et al. (2004), and Bar-Yosef and Garfinkel (2008: 79–80) and argue that the Acheulian site of Holon may be older than suggested.

In summary, the few Acheulian dates available seem to be problematic. It seems that the dates commonly underestimate the true ages of the Acheulian sites possibly because the relevant dating methods are limited and unreliable beyond the Acheulo-Yabrudian time range.

5.2.3. Mousterian dates

Early Middle Paleolithic Mousterian dates may provide an ante-quem date for the Acheulo-Yabrudian. The TL dates from Tabun D are as early as 270–250 ka (Mercier et al., 1995; Mercier and Valladas, 2003). The ESR dates of the same layer are younger in the order of 200 ka or later for the beginning of Tabun D (Grün and Stringer, 2000).

A recent summary of the TL and ESR chronology of Hayonim Cave (Mercier et al., 2007) suggests that the beginning of the Mousterian (layers F–E) at Hayonim Cave was at ca. 220 ka. The Acheulo-Yabrudian layer G (Bar-Yosef et al., 2006: 24) at the bottom of the sequence of Hayonim Cave was not dated. An average of U-series ages from the Mousterian of Nahal Aqev of 211 ± 19 (cf Bar-Yosef, 2000) was criticized by Porat et al. (2002). U-series dates on ostrich eggshell samples from the Mousterian site of Rosh Ein Mor are around 200 ka (Rink et al., 2002).

The ages discussed above indicate a start of the Mousterian around 220–200 ka that accords well with the latest dates we suggest for the AYCC.

6. Summary

The dating of Qesem Cave at present relies on U-series of speleothems from within the excavated sequence of the cave. The available results indicate that human occupation at Qesem Cave started between ~420 and ~320 ka and ended between ~220 and ~194 ka. The dated speleothem samples relevant for the human use of the cave are in direct contact with the archaeological layers. Preliminary results from a TL dating project currently underway including samples from the lower sequence support an early start for human occupation in the cave.

A broader view following the above survey of dates and the Qesem Cave dates would maintain that:

- The beginning of the Acheulo-Yabrudian Cultural Complex is not yet positively secured, but based on the above considerations it is expected to be around 400 ka.
- The end of the Acheulo-Yabrudian sequence is around 200 ka and possibly a little earlier.

The thick stratigraphic sequences of sites such as Qesem Cave, Tabun layer E and Hummal, and other Acheulo-Yabrudian sites in Israel and Syria and the radiometric dates available indicate a long time span for the Acheulo-Yabrudian Cultural Complex covering some 200 ka between the two major Paleolithic complexes, the Lower Paleolithic Acheulian and the Middle Paleolithic Mousterian.

Acknowledgments

The U-series dating project was supported by a grant of the Wenner Gren Foundation. Field work at Qesem Cave and laboratory work were supported by grants of the Israel Science Foundation,

CARE archaeological foundation, Leakey Foundation and the Thyssen Foundation.

We would like to thank N. Tepliakov, I. Segal, N. Shalev, G. Gerber and A. Vaks for helping with the U–Th dating at the Geological Survey of Israel.

Editorial handling by: D. Richards

References

Ayalon, A., Bar-Matthews, M., Sass, E., 1998. Rainfall–recharge relationships within a karstic terrain in the Eastern Mediterranean semi-arid region, Israel: $^{18}\delta$O and δD characteristics. Journal of Hydrology 207, 18–31.

Barkai, R., Gopher, A., Lauritzen, S.E., Frumkin, A., 2003. Uranium series dates from Qesem Cave, Israel, and the end of the Lower Palaeolithic. Nature 423, 977–979.

Barkai, R., Gopher, A., Shimelmitz, R., 2005. Middle Pleistocene blade production in the Levant: an Amudian assemblage from Qesem Cave, Israel. Eurasian Prehistory 3, 39–74.

Barkai, R., Lemorini, C., Shimelmitz, R., Lev, Z., Stiner, M., Gopher, A., 2009. A blade for all seasons: making and using Amudian blades at Qesem Cave, Israel. Human Evolution 24, 57–75.

Bar-Yosef, O., 1994. The Lower Paleolithic in the Near East. Journal of World Prehistory 8, 211–265.

Bar-Yosef, O., 1998. The chronology of the Middle Paleolithic of the Levant. In: Akazawa, T., Aoki, K., Bar-Yosef, O. (Eds.), Neanderthals and Modern Humans in Western Asia. Plenum, New York, pp. 39–56.

Bar-Yosef, O., 2000. The Middle and Early Upper Paleolithic in Southwest Asia and neighboring regions. In: Bar-Yosef, O., Pilbeam, D. (Eds.), The Geography of Neanderthals and Modern Humans in Europe and the Greater Mediterranean. Peabody Museum of Archaeology and Anthropology, Cambridge, MA, pp. 107–156, Appendix, pp., 1189–1197.

Bar-Yosef, O., Garfinkel, Y., 2008. The Prehistory of Israel. Ariel Publishing House, Jerusalem.

Bar-Yosef, O., Belfer-Cohen, A., Goldberg, P., Kuhn, S., Meignen, L., Vandermeersch, B., Weiner, S., 2006. Archaeological background to Hayonim Cave and Meged Rockshelter. In: Stiner, M.C. (Ed.), The Faunas of Hayonim Cave (Israel): a 200,000-year Record of Paleolithic Diet, Demography, and Society. Harvard University, Peabody Museum of Archaeology and Ethnography, Cambridge, MA, pp. 17–38.

Cheng, H., Edwards, R.L., Hoff, J., Gallup, C.D., Richards, D.A., Asmerom, Y., 2000. The half-lives of uranium-234 and thourium-230. Chemical Geology 169, 17–33.

Copeland, L., 2000. Yabrudian and related industries: the state of research in 1996. In: Ronen, A., Weinstein-Evron, M. (Eds.), Toward Modern Humans: Yabrudian and Micoquian, 400–50 kyears ago. BAR International Series 850, pp. 97–117.

Farrand, W.R., 1994. Confrontation of geological stratigraphy and radiometric dates from Upper Pleistocene sites in the Levant. In: Bar-Yosef, O., Kra, R. (Eds.), Late Quaternary Chronology and Paleoclimate of the Eastern Mediterranean. Radiocarbon, Arizona, 33–54.

Feraud, G., York, D., Hall, C.M., Goren, N., Schwarcz, H.P., 1983. ^{40}Ar/^{39}Ar age limit for an Acheulian site in Israel. Nature 304, 263–265.

Fischhendler, I., Frumkin, A., 2008. Distribution, evolution and morphology of caves in south-western Samaria, Israel. Israel Journal of Earth Sciences 57, 311–322.

Frumkin, A., Fischhendler, I., 2005. Morphometry and distribution of isolated caves as a guide for phreatic and confined paleohydrological conditions. Geomorphology 67, 457–471.

Frumkin, A., Karkanas, P., Bar-Matthews, M., Barkai, R., Gopher, A., Shahack-Gross, R., Vaks, A., 2009. Gravitational deformations and fillings of aging caves: the example of Qesem karst system, Israel. Geomorphology 106, 154–164.

Frumkin, A., Ford, D.C., Schwarcz, H.P., 1999. Continental oxygen isotopic record of the last 170,000 years in Jerusalem. Quaternary Research 51, 317–327.

Garrod, D.A.E., 1956. 'Acheuleo-Jabrudian' et 'Pre-Aurignacian' de la grotte du Taboun (Mont Carmel): étude stratigraphique et chronologique. Quaternaria 3, 39–59.

Garrod, D.A.E., 1970. Pre-Aurignacian and Amudian: a comparative study of the earliest blade industries of the Near East. In: Gripp, K., Schütrumpf, R., Schwabedissen, H. (Eds.), Frühe Menschheit und Umwelt. Böhlau Verlag, Köln, pp. 224–229.

Goren-Inbar, N., 1995. The Lower Paleolithic of Israel. In: Levy, T. (Ed.), The Archaeology of Society in the Holy Land. Leicester University Press, London, pp. 93–109.

Gopher, A., Barkai, R., Shimelmitz, R., Khalaily, M., Lemorini, C., Hershkovitz, I., Stiner, M., 2005. Qesem Cave: an Amudian site in Central Israel. Journal of the Israel Prehistoric Society 35, 69–92.

Grün, R., Stringer, C., 2000. Tabun revisited: revised ESR chronology and new ESR and U-series analyses of dental material from Tabun C1. Journal of Human Evolution 39, 601–612.

Grün, R., Stringer, C., Schwarcz, H., 1991. ESR dating of teeth from Garrod's Tabun cave collection. Journal of Human Evolution 20, 231–248.

Hennig, G.J., Hours, F., 1982. Dates pour le passage entre l'Acheuleen et le Paleolithique moyen a El Kowwm (Syrie). Paleorient 8, 81–83.

Jelinek, A.J., 1982. The Tabun Cave and Paleolithic Man in the Levant. Science 216, 1369–1375.

Jelinek, A.J., 1990. The Amudian in the context of the Mugharan tradition at the Tabun cave (Mt. Carmel), Israel. In: Mellars, P. (Ed.), The Emergence of Modern Humans. Edinburgh University Press, Edinburgh, pp. 81–90.

Karkanas, P., Shahack-Gross, R., Ayalon, A., Bar-Matthews, M., Barkai, R., Frumkin, A., Gopher, A., Stiner, M.C., 2007. Evidence for habitual use of fire at the end of the Lower Paleolithic: site formation processes at Qesem Cave, Israel. Journal of Human Evolution 53, 197–212.

Kaufman, A., Wasserburg, G.J., Porcelli, D., Bar-Matthews, M., Ayalon, A., Halicz, L., 1998. U–Th isotope systematics from the Soreq cave, Israel and climatic correlations. Earth and Planetary Science Letters 156, 141–155.

Lemorini, C., Stiner, M.C., Gopher, A., Shimelmitz, R., Barkai, R., 2006. Use-wear analysis of an Amudian laminar assemblage from the Acheuleo-Yabrudian of Qesem Cave, Israel. Journal of Archaeological Science 33, 921–934.

Le Tensorer, J.-M., Hauck, Th., Woitczak, D., Schmid, P., Schumann, D., Ismail-Meyer, K., Martineau, A.S., 2007a. Hummal et Nadaouiyeh (El Kowm, Syrie centrale), Resultats de la campagne 2007. http://elkowm.unibas.ch/Bilder/Publikationen/2007/RAP%20Fouille%2007.pdf.

Le Tensorer, J.-M., Jagher, R., Rentzel, P., Hauck, T., Ismail-Meyer, K., Pümpin, C., Woitczak, D., 2007b. Long-term site formation processes at the natural springs Nadaouiyeh and Hummal in the El Kowm oasis, Central Syria. Geoarchaeology 22 (6), 621–639.

Ludwig, K.R., 2003. Mathematical–statistical treatment of data and errors for ^{230}Th/U geochronology. Reviews in Mineralogy and Geochemistry 52, 631–656.

Marder, O., Khalaily, M., Rabinovich, R., Gvirtzman, G., Wieder, M., Porat, N., Ron, H., Bankirer, R., Saragusti, I., 1999. The Lower Paleolithic site of Revadim Quarry, preliminary results. Journal of the Israel Prehistoric Society 28, 21–53.

Marder, O., Milevski, Y., Rabinovich, R., 2007. Revadim Quarry. Excavations and Surveys in Israel 119. Israel Antiquities Authority. http://www.antiquities.org.il/home_heb.asp.

Maul, L.C., Smith, K.T., Barkai, R., Barash, A., Shahack-Gross, R., Gopher, A. Of men and mice at Middle Pleistocene Qesem Cave, Israel: small vertebrates, environment and biostratigraphy. Lecture delivered in the International Workshop on "Climatic Change in the Upper Jordan Valley between ca. 800 ka and 700 ka", Jerusalem, May 19–21, 2009, Journal of Human Evolution, in press (special issue).

McDermott, F., Grün, R., Stringer, C.B., Hawkesworth, C.J., 1993. Mass-spectrometric U-series dates for Israeli Neanderthal/early modern hominid sites. Nature 363, 252–255.

Mercier, N., Valladas, H., 1994. Thermoluminescence dates for the Paleolithic Levant. In: Bar-Yosef, O., Kra, R. (Eds.), Late Quaternary Chronology and Paleoclimate of the Eastern Mediterranean. Radiocarbon, Arizona, 13–20.

Mercier, N., Valladas, H.G., 2003. Reassessment of TL age estimates of burnt flints from the Paleolithic site of Tabun Cave, Israel. Journal of Human Evolution 45, 401–409.

Mercier, N., Valladas, H., Valladas, H.G., Reyss, J.-L., Jelinek, A.J., Meignen, L., Joron, L., 1995. TL dates of burnt flints from Jelinek's excavations at Tabun and their implications. Journal of Archaeological Science 22, 495–509.

Mercier, N., Valladas, H., Froget, L., Joron, L., Reyys, J.-L., Weiner, S., Goldberg, P., Meignen, L., Bar-Yosef, O., Belfer-Cohen, A., Chech, M., Kuhn, S., Stiner, M.C., Tillier, A.-M., Arenbsurg, B., Vandermeersch, B., 2007. Hayonim Cave: a TL-based chronology for the Levantine Mousterian sequence. Journal of Archaeological Science 34, 1064–1077.

Oxford Research Laboratory for Archaeology, 1990. Date list 4. Ancient TL 8, 43.

Pike, A.W.G., Pettitt, P.B., 2003. U-series dating and human evolution. Reviews in Mineralogy and Geochemistry 52, 607–629.

Porat, N., 2007. Luminescence and electron spin resonance dating. In: Chazan, M., Kolska-Horwitz, L. (Eds.), Holon, a Lower Paleolithic Site in Israel. American School of Prehistoric Research Bulletin 50. Peabody Museum of Archeology and Ethnology, Harvard University, Cambridge, MA., pp. 27–42.

Porat, N., Ronen, A., 2002. Luminescence and ESR age determinations of the Lower Paleolithic site Evron Quarry, Israel. Advances in ESR Applications 18, 123–130.

Porat, N., Zhou, L.P., Chazan, M., Noy, T., Howritz, L.K., 1999. Dating the Lower Paleolithic open-air site of Holon, Israel by luminescence and ESR techniques. Quaternary Research 51, 328–341.

Porat, N., Chazan, M., Schwarcz, H., Horwitz, L.K., 2002. Timing of the Lower to Middle Paleolithic boundary: new dates from the Levant. Journal of Human Evolution 43, 107–122.

Richards, D.A., Dorale, J.A., 2003. Uranium-series chronology and environmental applications of speleothems. Reviews in Mineralogy and Geochemistry 52, 407–460.

Rink, W.J., Richter, D., Schawrcz, H.P., 2002. Age of the Middle Paleolithic site of Rosh Ein Mor, Central Negev, Israel: implications for the age range of Early Levantine Mousterian of the Levantine Corridor. Journal of Archaeological Science 30, 195–204.

Rink, W.J., Schawrcz, H.P., 2005. Short contribution: ESR and uranium series dating of teeth from the Lower Paleolithic site of Gesher Benot Ya'aqov, Israel: confirmation of paleomagnetic age indications. Geoarchaeology 20, 57–66.

Rink, W.J., Schwarcz, H.P., Ronen, A., Tsatskin, A., 2004. Confirmation of a near 400 ka age for the Yabrudian industry at Tabun Cave, Israel. Journal of Archaeological Science 31, 15–20.

Ronen, A., Weinstein-Evron, M. (Eds.), 2000. Towards Modern Humans: Yabrudian and Micoquian, 400–50 kyears ago. BAR International Series 850.

Rust, A., 1950. Die Höhlenfunde von Jabrud (Syrien). Karl Wachholtz Verlag, Neumünster.

Schwarcz, H.P., 1980. Absolute age determination of archaeological sites by uranium series dating of travertines. Archaeometry 22, 3–24.
Schwarcz, H., Rink, W.J., 1998. Progress in ESR and U-Series chronology of the Levantine Paleolithic. In: Akazawa, T., Aoki, K., Bar-Yosef, O. (Eds.), Neanderthals and Modern Humans in Western Asia. Plenum, New York, pp. 57–68.
Shahack-Gross, R., Berna, F., Karkanas, P., Weiner, S., 2004. Bat guano and preservation of archaeological remains in cave sites. Journal of Archaeological Science 31, 1259–1272.
Stiner, M.C., Barkai, R., Gopher, A., 2009. Cooperative hunting and meat sharing 400–200 kya at Qesem Cave, Israel. Proceedings of the National American Academy of Science 106 (32), 13207–13212.
Vaks, A., 2008. Quaternary Paleoclimate of North-Eastern Boundary of the Saharan Desert: Reconstruction from Speleothems of Negev Desert, Israel. Unpublished PhD thesis. The Hebrew University of Jerusalem, 208 pp.
Vaks, A., Bar-Matthews, M., Ayalon, A., Schilman, B., Gilmour, M., Hawkesworth, C.J., Frumkin, A., Kaufman, A., Matthews, A., 2003. Paleoclimate reconstruction based on the timing of speleothem growth, oxygen and carbon isotope composition from a cave located in the 'rain shadow', Israel. Quaternary Research 59, 182–193.
Vaks, A., Bar-Matthews, M., Ayalon, A., Matthews, A., Frumkin, A., Dayan, U., Halicz, L., Almogi-Labin, A., Schilman, B., 2006. Paleoclimate and location of the border between Mediterranean climate region and the Saharo-Arabian desert as revealed by speleothems from the northern Negev Desert, Israel. Earth and Planetary Science Letters 249, 384–399.
Vaks, A., Bar-Matthews, M., Ayalon, A., Matthews, A., Halicz, L., Frumkin, A., 2007. Desert speleothems reveal climatic window for African exodus of early modern humans. Geology 35, 831–834.
Valladas, H., Mercier, N., Joron, J.-L., Reyss, J.-L., 1998. GIF laboratory dates for Middle Paleolithic Levant. In: Akazawa, T., Aoki, K., Bar-Yosef, O. (Eds.), Neanderthals and Modern Humans in Western Asia. Plenum, New York, pp. 69–76.
Weinstein-Evron, M., Tsatskin, A., Porat, N., Kronfeld, J., 1999. A $^{230}Th/^{234}U$ date for the Acheulo-Yabrudian layer in the Jamal Cave, Mount Carmel, Israel. South African Journal of Sciences 95, 186–188.